View Article Online / Journal Homepage / Table of Contents for this issue

J. Chem. Soc., Faraday Trans. 1, 1983, **79**, 417-430

Kinetic Study of the Electrolytic Oxidation of Manganese(II) to Manganese(III) in Sulphuric Acid

BY ANSELM T. KUHN*

Institute of Dental Surgery, 256 Gray's Inn Road, London WC1X 8LD

AND TERRY H. RANDLE

Swinburne Institute of Technology, P.O. Box 218, Hawthorn 3122, Australia

Received 22*nd April*, 1982

The oxidation of manganese(II) at a rotating oxide-covered platinum disc electrode has been studied, with additional data on glassy carbon. Data for the reduction of manganese(III) at the Pt electrode are also reported. Reaction orders in [Mn^{II}] and [Mn^{III}], as well as the effect of [SO_4^{2-}], are reported, as is the current efficiency for the oxidation process. It is shown, using partial current values obtained by chemical analysis, that Mn^{II} oxidation and the concurrent oxygen evolution do not proceed independently, and attempts to determine the rate of the former by subtraction of the rate of oxygen evolution in the absence of Mn^{II} leads to invalid results. The oxidation kinetics of Mn^{II} are controlled by formation of a film at the anode surface, and the role of this process is considered.

Manganese(III) is a highly oxidizing species in weakly complexing acid media with $E_f^{\ominus}$ (formal potential) = 1.56 V in 3 mol dm^{-3} $HClO_4$[1] and 1.488 V in 7.5 mol dm^{-3} H_2SO_4.[2] Consequently it has been used as a titrimetric agent in analytical chemistry.[3-5] More recently this ion has been utilized in indirect electrosynthesis for the specific oxidation of organic compounds, *e.g.* toluene to benzaldehyde[6] and aniline to *p*-benzoquinone.[7] The chemical oxidation of organic compounds by solutions of Mn^{III} has been reviewed by Waters.[8] It is in the context of indirect electro-organic synthesis that this study of the electrolytic oxidation of Mn^{II} to Mn^{III} at a platinum anode in sulphuric acid has been undertaken.

The electrolytic generation of strong oxidizers in aqueous solution is complicated by the following associated factors, each of which must be taken into account in any valid kinetic study. (i) At the high positive potentials required almost all metal anodes are covered with an oxide layer. Both the nature and thickness of this layer can influence the kinetics and mechanism of the anodic reaction. (ii) The anodic reaction under study is accompanied by the oxidation of water (oxygen evolution), *i.e.* the observed current is the sum of two partial currents. It cannot be automatically assumed that the two anodic reactions proceed independently, and the practice adopted by some workers of running a 'blank' (oxygen evolution alone) and then measuring the additional current after addition of the redox system is known to give unreliable results. (iii) The oxidizer formed is thermodynamically unstable toward chemical reduction by water.

The oxidation of Mn^{II} to Mn^{III} is further complicated by the possible formation of higher oxidation states, namely Mn^{IV} and Mn^{VII} in acidic solution (pH < 0),[9,10] and the disproportionation of Mn^{3+}:[11]

$$2Mn^{3+}_{(aq)} + 2H_2O \rightleftharpoons Mn^{2+}_{(aq)} + MnO_{2(s)} + 4H^+_{(aq)} \; (K = 10^9).$$

Hydrolysis of Mn^{3+} may also be significant.[12]

Published on 01 January 1983. Downloaded by Michigan State University on 22/01/2016 01:09:22.

View Article Online

Published on 01 January 1983. Downloaded by Michigan State University on 22/01/2016 01:09:22.

Selim and Lingane[13] demonstrated that stable solutions of Mn^{III} were formed in concentrated sulphuric acid (4.6-7.2 mol dm^{-3}) in the presence of an excess of Mn^{II} (*e.g.* ten-fold). They also found the rate of reduction of Mn^{III} by water to be a minimum in 6.3 mol dm^{-3} H_2SO_4 (half-life = 30 months). Stabilization of Mn^{III} by complexation with stronger ligands than SO_4^{2-} is of little practical interest because of the corresponding decrease in oxidizing power of such solutions.[14]

The electrolytic oxidation of Mn^{II} to Mn^{III} has been studied mainly in acidic sulphate solutions,[13,15-24] in phosphate[25,26] and pyrophosphate,[3,15,27,28] and in mixed sulphate–phosphate solutions.[15,20,29] A variety of anodes other than platinum have been shown to allow oxidation, *e.g.* PbO_2,[19,30] Au,[20,24] boron carbide,[22] paraffin-impregnated carbon[22] and glassy carbon.[24] Most studies have sought only to measure and optimize current efficiency for Mn^{III} generation, and provide no fundamental kinetic data. In general this species can be formed with high current efficiency (> 99%) under conditions which stabilize Mn^{III} and minimize the oxidation of water.[13,22,24]

In contrast the kinetics of the electrolytic reduction of Mn^{III} have been more thoroughly studied, factor (ii) above not being significant in this case. Vetter and Manecke[2] made a comprehensive investigation of the reduction reaction at a rotating platinum electrode in 7.5 mol dm^{-3} H_2SO_4. They concluded from reaction-order studies that the mechanism was simply

$$Mn^{3+}_{(aq)} + e \rightleftharpoons Mn^{2+}_{(aq)}$$

and determined the standard rate constant (k_s) and transfer coefficient (α_c) of the charge-transfer process to be $(1.0\text{-}1.5) \times 10^{-5}$ cm s^{-1} (with respect to the geometric electrode area) and 0.28, respectively. The low value of the transfer coefficient was substantiated by later workers.[31-33] In a recent study of the electrolytic generation of Mn^{III} in 7.5 mol dm^{-3} H_2SO_4, Bishop and Cofré[24] have reported anodic transfer coefficients (α_a) of 0.38-0.47, with $k_s = 3.4 \times 10^{-5}$-1.1×10^{-4} cm s^{-1} (geometric area) on anodes of platinum, gold and glassy carbon. These α_a values are much lower than expected from the α_c values of Vetter and others.

Note that the reduction of Mn^{III} can also proceed on an oxide-covered electrode, even in the case of platinum, a fact not taken into account in previous studies of the Mn^{III}/Mn^{II} system. If the oxide layer constitutes a barrier to charge transfer, the kinetics of the oxidation reaction cannot be deduced from a study of the reduction reaction, since it cannot be assumed that $\alpha_a + \alpha_c = 1$,[34,35] as indicated by the theory of electrodics for a simple, one-electron, charge-transfer process. In this study the reaction kinetics have been studied under conditions of constant Pt oxide thickness and history, thereby eliminating a factor which will have affected the results of earlier workers.

EXPERIMENTAL

Solutions of Mn^{III} in the presence of Mn^{II} were formed by chemical reaction between $KMnO_4$ and $MnSO_4$ in sulphuric acid:

$$4Mn^{II} + MnO_4^- + 8H^+ \rightarrow 5Mn^{III} + 4H_2O.$$

A.R. grade chemicals were used throughout, and the final concentration of H_2SO_4 was always 6.15 mol dm^{-3}, *i.e.* within the range of maximum kinetic stability of Mn^{III}.[13] Permanganate stock solution was made up and stored in such a way as to avoid formation of MnO_2,[36] which catalyses the disproportionation of Mn^{III}.[37] Chemical analysis of the manganic–manganous solutions showed the Mn^{III} and Mn^{II} contents to be as expected from the reaction stoichiometry. Solution stability was checked initially by u.v. spectroscopy; all Mn^{III}–Mn^{II} solutions were observed to

View Article Online

Published on 01 January 1983. Downloaded by Michigan State University on 22/01/2016 01:09:22.

be stable in 6.15 mol dm^{-3} H_2SO_4 over the period of experimentation (several days). All sulphuric acid used as supporting electrolyte was purified by pre-electrolysis.

Steady-state current–voltage data were recorded at a platinum rotating-disc electrode, the platinum disc (geometric area = 0.0305 ± 0.0003 cm^2) being encased in a PTFE shroud of conventional bell-shaped design. The potential of the disc electrode was controlled with a Utah Electronics potentiostat (model 0152). All potentials are expressed relative to the Hg/Hg_2SO_4, 6.15 mol dm^{-3} H_2SO_4 reference system unless stated otherwise. All electrochemical measurements were made at 25 °C in a water-jacketted cell. The auxiliary electrode was also of platinum.

In order to study the kinetics of the redox system under conditions of constant thickness of platinum oxide, the following potential programme was applied to the working electrode in recording each oxidation or reduction voltammogram.

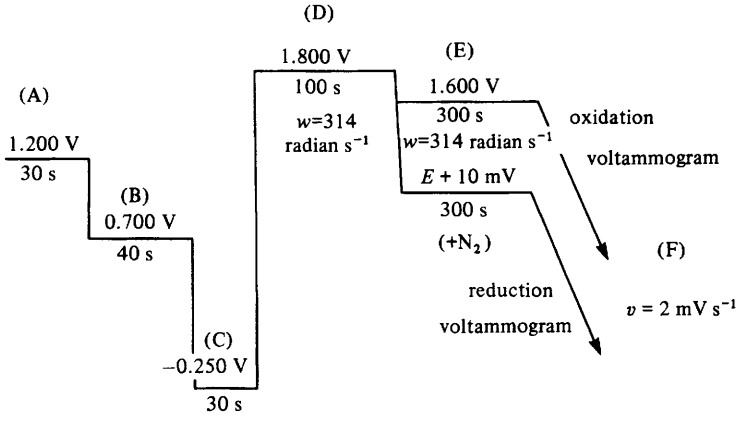

Steps A and B constitute pre-cleaning steps, while step C reduces any existing oxide on the electrode surface. In step D the oxide layer is formed to a constant thickness as measured by $Q_O/2Q_H$, where Q_O is the charge required to reduce the oxide layer, and Q_H is the charge required to form a monolayer of adsorbed hydrogen on the electrode surface. Oxidation at 1.800 V for 100 s forms only that oxide of platinum known as the α-oxide (Shibata's nomenclature[38]). This oxide forms as only a very thin layer, thickness < 1.0 nm; in this work the thickness was constant at $Q_O/2Q_H \approx 1.8$ (≈ 0.6 nm assuming the α-oxide is PtO with a density of 13.3 g cm^{-3} [39]).

After oxide formation the relevant oxidation or reduction voltammogram was recorded (step F), the potential scan always starting at the most anodic limit which was always below (step E) that of oxide formation. This procedure prevents further oxide growth during step E and the potential scan,[40] while the large hysteresis in oxide reduction does not allow oxide reduction at potentials above 0.4 V in 6.15 mol dm^{-3} H_2SO_4. Polarization curves for the supporting electrolyte alone were also recorded according to the above potential programme, as the kinetics of the oxygen evolution reaction (o.e.r.) are dependent on the thickness of the α-oxide layer.[41-43] Oxide coverage and electrode area, as determined from Q_H by the method of Biegler *et al.*,[44] were checked periodically throughout, since repetitive cycling of a platinum electrode between the potential limits of oxide formation and reduction may cause roughening of the surface.[45]

A limited number of experiments with glassy carbon (Tokai Electrode Manufacturing, Japan, type G.C. 30S) are also reported. These were polished down to 1 μm diamond-paste finish and conditioned with a potential pulse programme similar to that used for Pt (−0.80 V, 60 s; +1.60 V, 120 s; +0.700 V, 120 s, followed by the voltammogram).

View Article Online

RESULTS AND DISCUSSION

REDUCTION OF Mn^{III} IN SULPHURIC ACID

As the current–voltage characteristics of the oxidation and reduction reaction are markedly different at high overpotentials, a summary of the kinetics of the reduction reaction under conditions of constant oxide coverage is presented for comparison, although the kinetics are in general agreement with those reported by Vetter and Manecke.[2]

Typical reduction voltammograms are shown in fig. 1. At low overpotentials the current (I) is charge-transfer controlled, being independent of electrode rotation rate (w). With increase in overpotential the current is subject to mass-transport control, and eventually attains a well defined limiting value (I_L) which varies linearly with $(w)^{\frac{1}{2}}$ and $[Mn^{III}]$. The limiting-current region overlaps that for platinum oxide reduction,

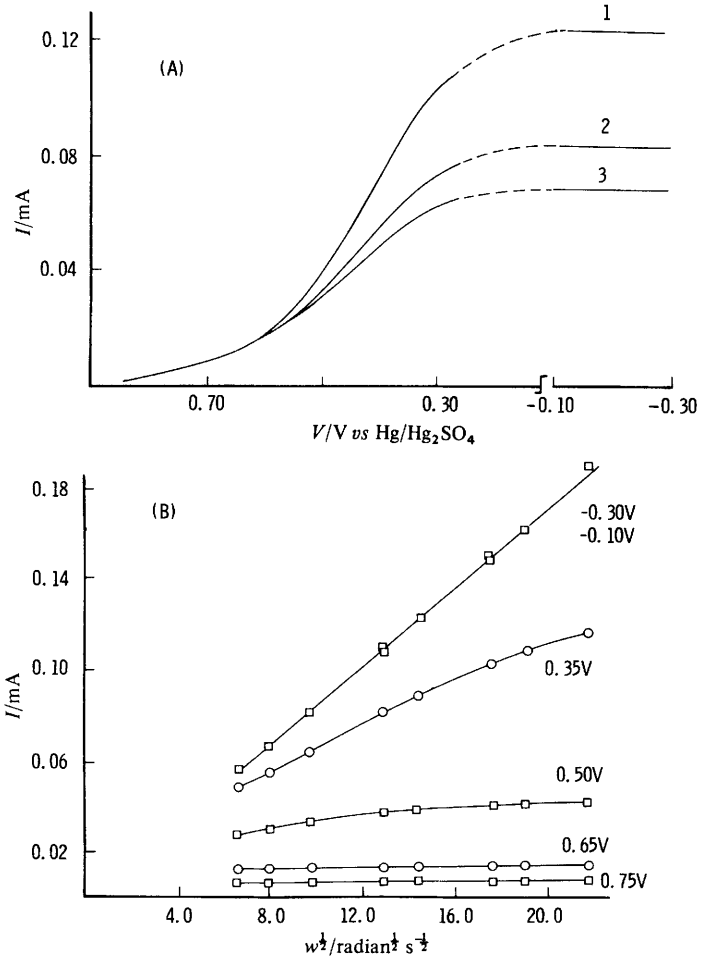

FIG. 1.—The reduction of Mn^{III} in 6.15 mol dm^{-3} H_2SO_4 at the platinum rotating-disc electrode. (A) Reduction voltammograms, $w = 209$ (1), 95 (2), and 65 (3) radian s^{-1}. (B) Variation of reduction current with electrode rotation rate. ($[Mn^{II}] = 38$ mmol dm^{-3}, $[Mn^{III}] = 15$ mmol dm^{-3}, $v = 2$ mV s^{-1}.)

Published on 01 January 1983. Downloaded by Michigan State University on 22/01/2016 01:09:22.

View Article Online

hence to record accurate limiting currents it is necessary to measure the current at a potential at which the electrode is fully reduced, *e.g.* 0 V. The diffusion coefficient (D) of Mn^{III} in 6.15 mol dm^{-3} H_2SO_4 was determined as $(1.93 \pm 0.06) \times 10^{-6}$ cm^2 s^{-1} from the gradients of the I_L against $\sqrt{w}$ and I_L against $[Mn^{III}]$ plots ($[Mn^{III}]$ varied from 0.5 to 50 mmol dm^{-3}) according to the Levich equation ($I_L = 0.62\, FAD^{\frac{2}{3}} \times v^{-\frac{1}{6}}[Mn^{III}]w^{\frac{1}{2}}$). The kinematic viscosity (v) of 6.15 mol dm^{-3} H_2SO_4 at 25 °C was determined as $(2.012 \pm 0.005) \times 10^{-2}$ cm^2 s^{-1}.

Reaction-order studies in which $[Mn^{III}]$ was varied (0.5, 1.0, 2.0, 5.0, 10.0, 20.0 and 50.0 mol dm^{-3}) at constant $[Mn^{II}]$ (100 mmol dm^{-3}) indicated first-order kinetics in $[Mn^{III}]$

$$i.e. \left[\frac{\partial \ln I}{\partial \ln (I_L - I)}\right]_{V,\, w,\, [Mn^{II}]} = 1$$

for $\eta > 60$ mV. Similarly variation in $[Mn^{II}]$ from 8.4 to 198.4 mmol dm^{-3} in 9 steps, while maintaining $[Mn^{III}]$ constant at 2 mmol dm^{-3}, showed the reduction current to be zero order in Mn^{II}. Both results indicate the absence of any mechanism involving disproportionation of Mn^{III} as a preceding step.

For a first-order, one-electron reduction process proceeding under joint mass-transport–charge-transfer control, the polarization curve at high overpotentials ($|\eta| > 60$ mV) may be described as

$$\eta = \frac{RT}{\alpha_c F} \ln i_0 + \frac{RT}{\alpha_c F} \ln [(I_L - I)/II_L] \qquad (1)$$

in the region $0.05 < I/I_L < 0.95$. A plot of η against $\ln [(I_L - I)/II_L]$ thus gives α_c and i_0 (the exchange current). The standard rate constant (k_s) may be obtained from

$$i_0 = Fk_s A[Mn^{III}]^{1-\alpha_c}[Mn^{II}]^{\alpha_c} \qquad (2)$$

where A is now the real electrode area as determined from Q_H (0.301 cm^2). Analysis of the polarization curves for the above solutions of Mn^{III} according to eqn (1) and (2) gave $\alpha_c = 0.22 \pm 0.01$ and $k_s = (2.52 \pm 0.05) \times 10^{-6}$ cm s^{-1}.

The manganous ion associates with SO_4^{2-} in sulphate solutions [$K_{stab}(MnSO_4)$ = 132-200].[46, 47] It is likely therefore that the smaller, highly charged Mn^{3+} species will be more strongly complexed; *i.e.* it is unlikely that the electroactive species is $Mn^{3+}_{(aq)}$. To examine the influence of $[SO_4^{2-}]$ on the reduction kinetics, voltammograms were recorded in four perchloric acid solutions (6.0 mol dm^{-3}), each being 0.013 mol dm^{-3} in Mn^{II} and 0.004 mol dm^{-3} in Mn^{III} and containing excess total SO_4^{2-} (0.04, 0.06, 0.08 and 0.1 mol dm^{-3}). The parameters $E_{\frac{1}{2}}$, k_s, α_c and i_L were independent of sulphate concentration, remaining constant at 0.395 ± 0.004 V, $(3.1 \pm 0.05) \times 10^{-6}$ cm s^{-1}, 0.20 ± 0.01 and 1.25 ± 0.03 mA cm^{-2}, respectively. It is unlikely then that there is participation of SO_4^{2-} in the reduction reaction, either directly or in a coupled pre-equilibrium step. At sulphate concentrations below 0.04 mol dm^{-3} there is a decrease in k_s and $E_{\frac{1}{2}}$ with decreasing sulphate content, but such solutions are unstable with respect to disproportionation, the rate of MnO_2 precipitation increasing with decreasing sulphate concentration. Similarly, the instability of Mn^{III} at acid concentrations < 6 mol dm^{-3} does not permit investigation of the reaction order with respect to $[H^+]$. For these and similar reasons, the scope of the reaction-order investigation appears to be constrained within the limits explored here.

Published on 01 January 1983. Downloaded by Michigan State University on 22/01/2016 01:09:22.

View Article Online

Published on 01 January 1983. Downloaded by Michigan State University on 22/01/2016 01:09:22.

OXIDATION OF Mn^{II} IN 6.15 mol dm^{-3} H_2SO_4

Fig. 2 shows a typical voltammogram for the oxidation of a Mn^{II} solution at the rotating-disc electrode. For convenience in subsequent discussion, the polarization curve is divided into potential regions (I, II, III and IV) as shown.

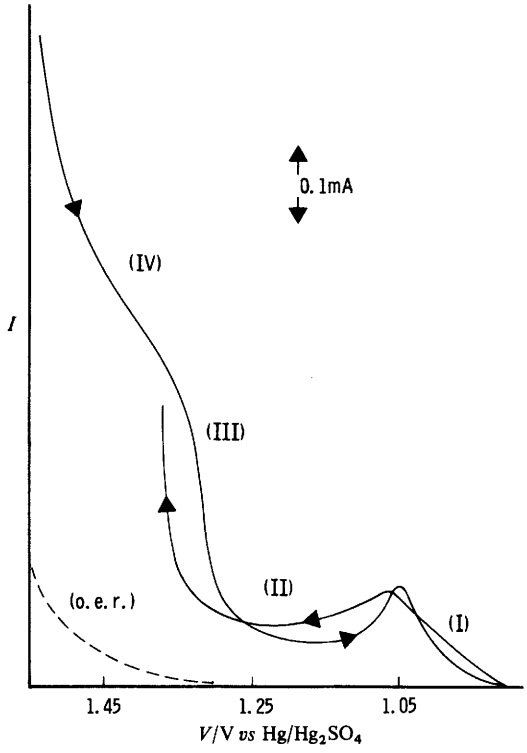

FIG. 2.—Voltammogram for the oxidation of Mn^{II} in 6.15 mol dm^{-3} H_2SO_4 at the platinum rotating-disc electrode. Roman numerals identify various regions referred to in the text. ($[Mn^{II}] = 82$ mmol dm^{-3}, $[Mn^{III}] = 2$ mmol dm^{-3}, $w = 314$ radian s^{-1}, $v = 2$ mV s^{-1}.)

CURRENT-EFFICIENCY STUDIES UNDER POTENTIOSTATIC CONDITIONS

The true current efficiency for the oxidation of Mn^{II} to Mn^{III} is of both practical and theoretical importance.

The potentiostatic data shown in fig. 3 represent:

$$\mathscr{F} = Q_{Mn}/Q_t \tag{3}$$

where $\mathscr{F}$ is the current efficiency, Q_{Mn} is the coulombic charge (assuming $n = 1$) required to form the Mn^{III} from Mn^{II} and Q_t is the total coulombic charge passed in time t. The former species was determined in this work by chemical analysis in which an aliquot of the electrolyte solution was withdrawn, allowed to react with excess standardised Fe^{II} and back-titrated with $KMnO_4$. A u.v. analysis of the electrolyte at each potential failed to indicate the presence of any other oxidation states of Mn,

View Article Online

Published on 01 January 1983. Downloaded by Michigan State University on 22/01/2016 01:09:22.

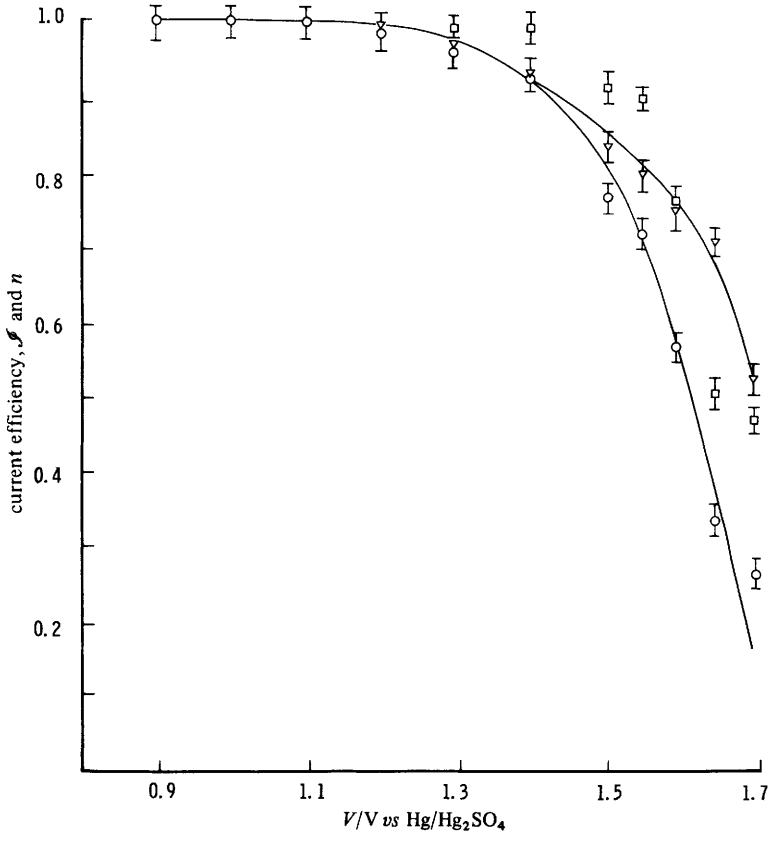

FIG. 3.—Current efficiency plotted against oxidation potential for Mn^{II} oxidation at the platinum rotating-disc electrode in 6.15 mol dm^{-3} H_2SO_4: ▽, actual current efficiency; ○, current efficiency assuming the oxidation of Mn^{II} and H_2O proceed independently; □, number of electrons (n) involved in the oxidation process calculated from the same assumption. ($[Mn^{II}] = 66$ mmol dm^{-3}, $w = 314$ radian s^{-1}).

notably Mn^{IV} or Mn^{VII}. These species would be expected[13] to be unstable in the presence of Mn^{II}, and strong sulphuric acid and would react chemically to form the Mn^{III}. At lower rotation rates, as implied by fig. 4, current efficiency falls off.

Investigation of the electrode kinetics of simultaneously occurring processes (since oxygen evolution occurs here with Mn^{II} oxidation) is a problem which is often avoided by workers precisely because of the difficulties. Some investigators have assumed that the kinetics and rate of one process (*i.e.* oxygen evolution) are unaffected by the introduction of the second, such as Mn^{II} oxidation.

If this were true, one could write

$$Q_t = Q_{Mn} + Q'_{o.e.r.} = Q_{Mn} + Q_{o.e.r.} \quad (4)$$

where Q_{Mn} is the charge consumed in oxidation of Mn^{II} to Mn^{III} and $Q'_{o.e.r.}$ and $Q_{o.e.r.}$ are the charges required for oxygen evolution in the absence and presence of Mn^{II}, respectively.

Because, in the present work, Q_{Mn} is known by chemical analysis, we can compare the value, at each potential, with the value one might obtain using the assumption and

View Article Online

equation above. Fig. 3 shows the true current efficiency given by expression (3), and also the imputed current efficiency which would arise if one assumed the two reactions to proceed independently [expression (4)]. The true current efficiency is considerably higher than the imputed value, and it is quite clear that (especially in the critical potential range 1.5-1.7 V) there is no justification for the latter assumption. Another way of showing how this procedure can mislead is also shown in fig. 3 by plotting the n values for Mn^{II} oxidation, again with the assumption that the two reactions proceed independently:

$$n = \frac{Q_t - Q'_{\text{o.e.r.}}}{Q_{\text{Mn}}}. \qquad (5)$$

Expression (5) is different from (3), and the two might be termed 'true' and 'apparent' current efficiency. The resulting n values of less than unity are seen to be the artefacts of this erroneous assumption, since from analytical data it is clear that only a single electron is involved. The suppression of the o.e.r. by Mn^{II} may result from adsorption of the ionic species on the electrode surface, and a similar but more marked effect has been observed by us with respect to Ce ions. While clearly visible at potentials anodic to 1.5 V (fig. 3), it is quite possible that the effect sets in even below these values, although confirmation of this would call for more sensitive techniques than those used here.

KINETICS OF OXIDATION

Fig. 4 and 5 show the dependence of the oxidation current at various potentials on w and $[Mn^{II}]$. In fig. 5 the expected mass-transport-limited current for a one-electron oxidation is also included for comparison, being calculated from the Levich equation on the assumption that $D_{Mn^{II}} = D_{Mn^{III}}$. In region I (*cf.* fig. 2) the current appears as a simple charge-transfer current, increasing with potential and being independent of w. Within this region the current shows a first-order dependence on $[Mn^{II}]$

$$i.e. \quad \left[\frac{\partial \ln I}{\partial \ln [Mn^{II}]}\right]_{V,[Mn^{III}]} = 1 \ (\eta > 60 \text{ mV}).$$

$[Mn^{II}]$ varied from 1.4 to 198.4 mmol dm^{-3}, $[Mn^{III}] = 2.0$ mmol dm^{-3} and has zero-order dependence on $[Mn^{III}]$ and $[SO_4^{2-}]$ for all solutions where $[SO_4^{2-}] \gg [Mn^{III}]$ or $[Mn^{II}]$. In the sulphate studies, the solutions were, as previously, 6.0 mol dm^{-3} $HClO_4$ with added Na_2SO_4. It can be concluded from these reaction-order studies and those of the preceding section that the electrode reaction is best represented by

$$Mn(SO_4)_x^{(3-2x)+} + e \rightleftharpoons Mn(SO_4)_x^{(2-2x)+} \ (x \geqslant 1).$$

Once all available Mn has been thus complexed, zero order in $[SO_4^{2-}]$ is implicit.

The current plateau in section II does not result from mass-transport limitation. The current is much smaller than the calculated I_L ($n = 1$), is independent of electrode rotation frequency and is not linearly proportional to $[Mn^{II}]$. These observations together with the unusual current peak (region I-II) indicate the occurrence of a current-inhibiting process at the potentials concerned. Similarly in section III the current is not a steady-state current at $v = 2$ mV s^{-1}; on stopping the scan the current slowly decreased to a steady value over a period of minutes.

In region IV the Mn^{II} oxidation current, although not completely independent of potential, tends to a limiting value and is essentially linearly dependent on $w^{\frac{1}{2}}$ and $[Mn^{II}]$ (fig. 4 and 5). However, for the following reasons it is difficult to relate the limiting current to known conditions of laminar flow. (i) Coevolution of oxygen enhances transport of Mn^{II} to the electrode, this effect becoming more significant with

Published on 01 January 1983. Downloaded by Michigan State University on 22/01/2016 01:09:22.

View Article Online

Published on 01 January 1983. Downloaded by Michigan State University on 22/01/2016 01:09:22.

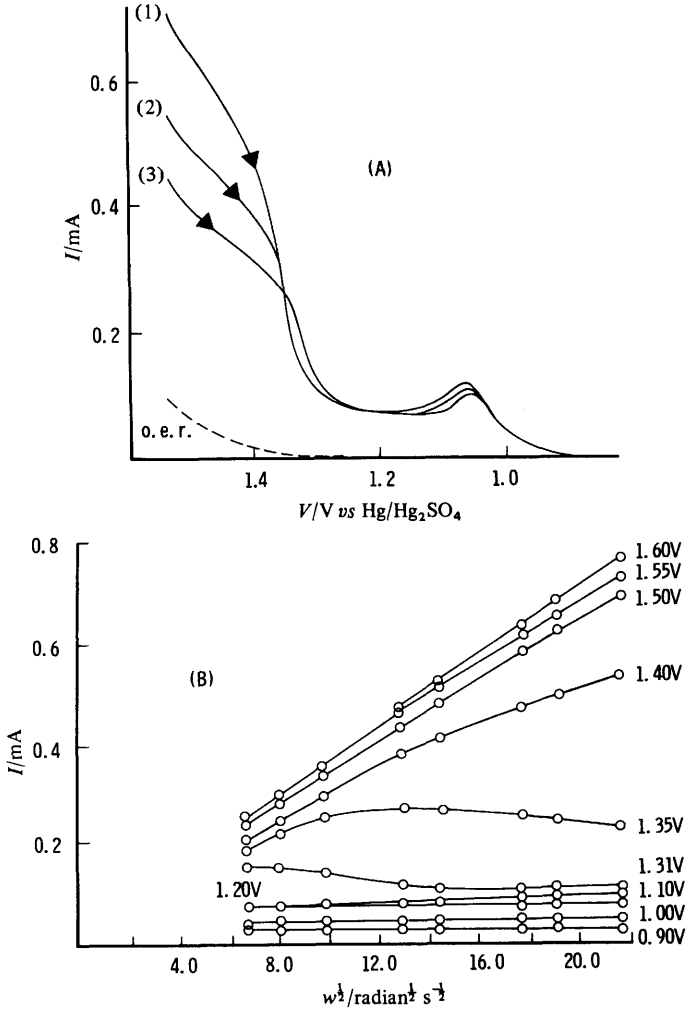

FIG. 4.—Influence of electrode rotation rate on Mn^{II} oxidation currents in 6.15 mol dm^{-3} H_2SO_4. (A) Oxidation voltammograms at $w = 314$ (1), 168 (2) and 96 (3) radian s^{-1}. (B) Test for mode of kinetic control. ($[Mn^{II}] = 55$ mmol dm^{-3} $[Mn^{III}] = 1.5$ mmol dm^{-3}, $v = 2$ mV s^{-1}.)

decreasing w and $[Mn^{II}]$. (ii) As shown by the current-efficiency studies, determination of $I_{Mn^{II}}$ as $I_t - I'_{o.e.r.}$ underestimates the true oxidation current above 1.5 V. (iii) With increasing $[Mn^{II}]$ the current inhibiting phenomenon of regions II-III extends to more anodic potentials, being responsible for the curvature in the I against $[Mn^{II}]$ plot at 1.600 and 1.500 V. Conversely with decreasing $[Mn^{II}]$ current inhibition becomes less directly apparent, and at concentrations below 3 mmol dm^{-3} the current plateau of section II is not observable on the oxidation voltammogram.

For $[Mn^{II}] < 50$ mmol dm^{-3} the limiting currents of section IV occur around 1.4 V. Under these conditions the experimental current shows reasonable agreement with the calculated limiting current ($n = 1$), *e.g.* $I_{expt}/I_{calc} = 1.0$-1.3 for $3 < [Mn^{II}]/\text{mmol dm}^{-3} < 40$. Owing to effects (i)–(iii) above it is not possible to

View Article Online

Published on 01 January 1983. Downloaded by Michigan State University on 22/01/2016 01:09:22.

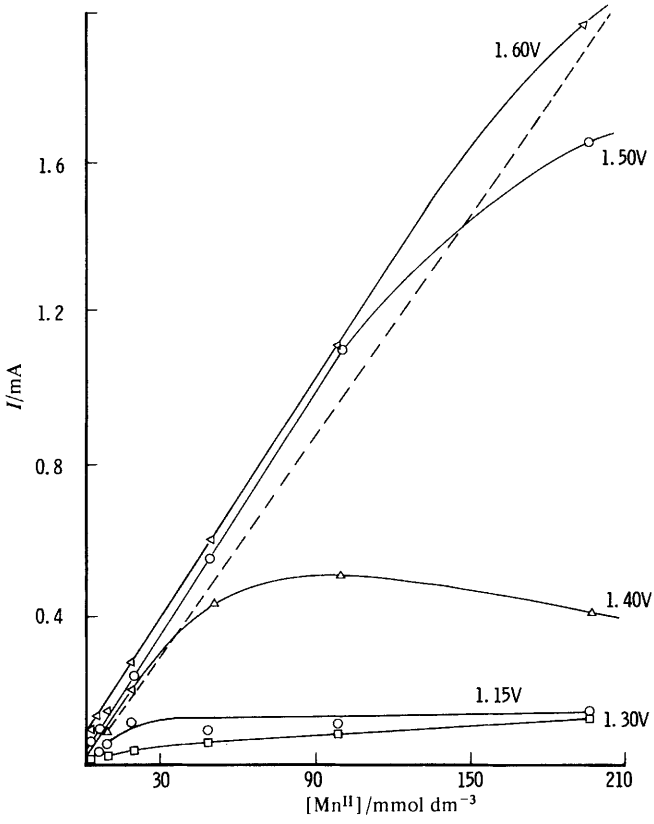

FIG. 5.—Oxidation of Mn^{II} in 6.15 mol dm^{-3} H_2SO_4. Variation of oxidation current in potential regions II-IV (fig. 2) with the concentration of Mn^{II}: (----) calculated limiting current for a one-electron mass-transport-controlled reaction. ($[Mn^{III}] = 2$ mmol dm^{-3}, $w = 314$ radian s^{-1}.) (These potential regions are dependent on $[Mn^{II}]$, as discussed in the text.)

decide if formation of higher oxidation states is occurring at higher potentials. For example at 1.600 V I_{expt}/I_{calc} decreases from 7.2 ($[Mn^{II}] = 1.4$ mmol dm^{-3}) to 1.0 ($[Mn^{II}] = 198.4$ mmol dm^{-3}).

Cyclic voltammetry at a glassy carbon anode (geometric area = 0.126 cm^2) was used to examine further the unusual current variation in region II, and to demonstrate that such behaviour was not peculiar to platinum. The same current plateau has also been observed in this laboratory with PbO_2 anodes. Voltammograms were recorded over a range of potential sweep rates (2-200 mV s^{-1}), the variation in observed behaviour being illustrated in fig. 6. The essential features are the shift to more positive potentials and the gradual disappearance of the current peak on the anodic scan with increasing scan rates, together with the replacement of the anodic peak on the cathodic scan by a cathodic peak at $v > 20$ mV s^{-1}.

The observed current–potential behaviour in region II under steady-state or transient conditions is consistent with the formation of a poorly conducting film of a manganese compound on the electrode surface, the film being formed by chemical reaction at the electrode surface. In terms of the film hypothesis the features of the

View Article Online

Published on 01 January 1983. Downloaded by Michigan State University on 22/01/2016 01:09:22.

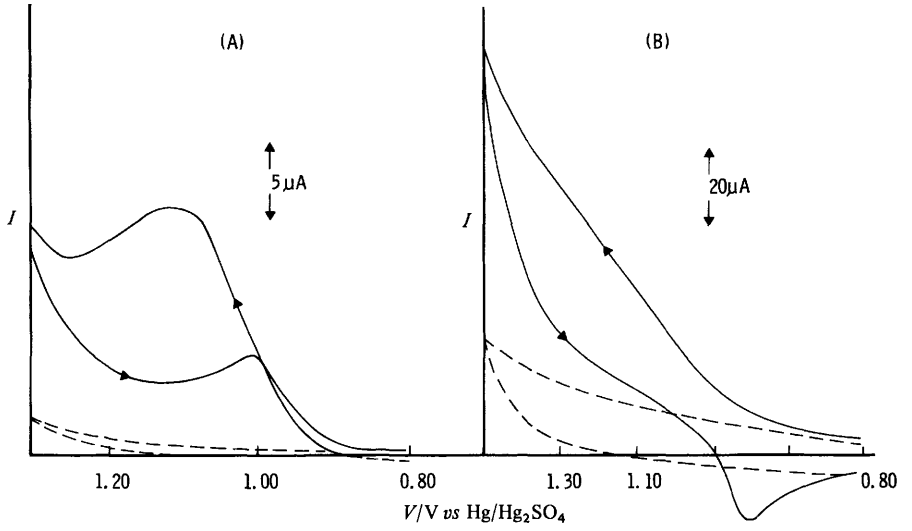

FIG. 6.—Cyclic voltammograms for the oxidation of Mn^{II} at a glassy carbon electrode in 6.15 mol dm^{-3} H_2SO_4 ($[Mn^{II}] = 18$ mmol dm^{-3}.) (A) $v = 2$ mV s^{-1}; (B) $v = 200$ mV s^{-1}.

steady-state voltammograms arise as follows. Beginning at the rest potential and on increasing the potential in the anodic direction, the current is initially charge-transfer controlled and increases with potential in the usual way. At *ca.* 1.05 V film formation occurs and the current decreases (anodic peak) to a steady-state 'limiting' value (region II). That the current does not decrease to zero suggests that the film is being continuously removed and reformed, the manganese compound being either soluble in H_2SO_4 or unstable in the presence of an excess of Mn^{II}. Hence the plateau current in region II is probably determined by the rate of film 'dissolution'. With further increase in potential the film begins to oxidize. When the rate of oxidation (plus dissolution) is greater than that of film formation, film coverage decreases and the current increases (region III) to an essentially mass-transport-controlled value (region IV). Increased mass transport will also increase the rate of dissolution of a poorly soluble film at the anode surface.

The hysteresis shown in fig. 2 can also be explained in terms of the existence of the current-inhibiting film. Similarly, the anodic peak at *ca.* 1.10 V on the steady-state oxidation voltammogram recorded by scanning the potential in the cathodic direction (fig. 2) occurs when the rate of film formation becomes less than that of 'dissolution', coverage decreases and the current increases to the normal charge-transfer-controlled value. The cyclic voltammetric studies show film removal to occur by 'dissolution' rather than electrochemical reduction. The small cathodic peak [fig. 6(B)] present at sweep rates above 20 mV s^{-1} is not apparent at lower sweep rates, suggesting it results from reduction of dissolved film species. At the lower rates of potential variation the solution species diffuse away from the electrode before it can be reduced. Similarly if the glassy carbon-disc electrode is rotated at 314 radian s^{-1} (3000 rev.min^{-1}) the cathodic peak is absent up to $v = 50$ mV s^{-1}.

The cyclic voltammetric data (fig. 6) and the steady-state data (fig. 4 and 5) are consistent with film formation *via* a coupled chemical reaction. As shown in fig. 6 the anodic peak on the anodic scan becomes less significant with increasing v, and is not

View Article Online

Published on 01 January 1983. Downloaded by Michigan State University on 22/01/2016 01:09:22.

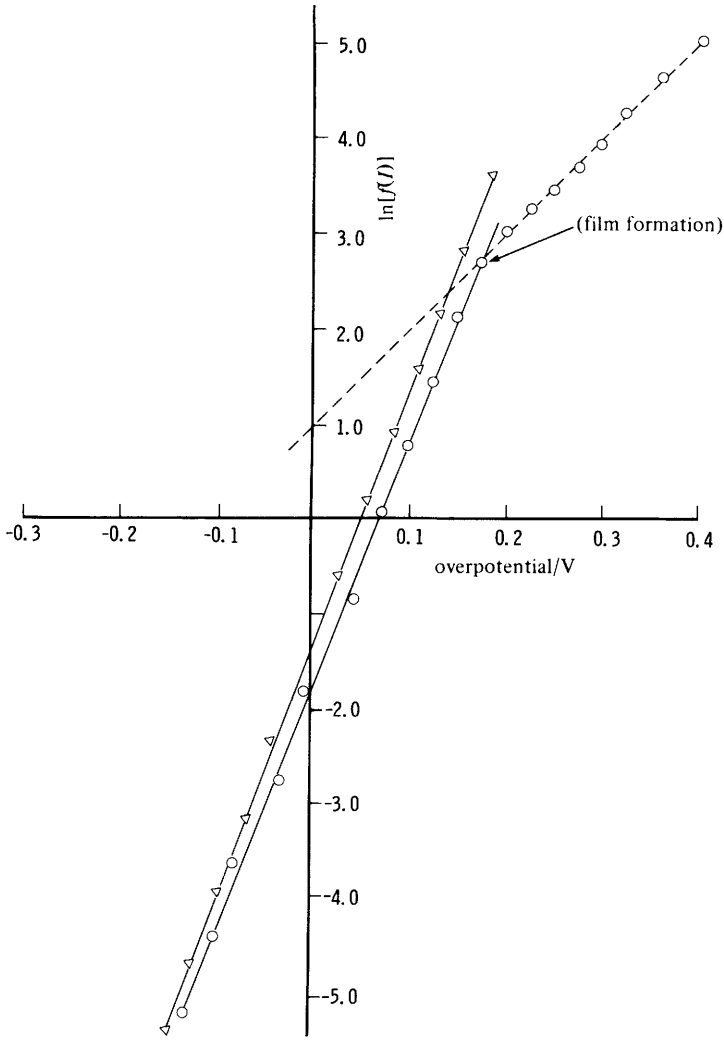

FIG. 7.—Allen–Hickling plots for the Mn^{III}/Mn^{II} system in 6.15 mol dm^{-3} H_2SO_4 at the Pt rotating-disc electrode: ○, $[Mn^{II}] = 5.4$ mmol dm^{-3}, $[Mn^{III}] = 2.0$ mmol dm^{-3}; ▽, $[Mn^{II}] = 18.4$ mmol dm^{-3}, $[Mn^{III}] = 2.0$ mmol dm^{-3}; $w = 314$ radian s^{-1}. $f(I) = I/[(1 - I/I_{L,Mn^{II}}) - (1 + I/I_{L,Mn^{III}}) \exp - F\eta/RT]$.

discernable at 200 mV s^{-1}. The finite rate of the chemical reaction dictates smaller film coverage at high sweep rates. The non-linear current variation in fig. 4 and 5 results because the potential at which the film oxidation rate exceeds (region III) that of film formation becomes more anodic with increasing w (at constant $[Mn^{II}]$) and with increasing $[Mn^{II}]$ (constant w); *i.e.* the higher the concentration of the chemically active product of the electrode reaction at the electrode surface, the greater the rate of film formation. Possible chemical reactions may involve hydrolysis of active Mn^{III}, or disproportionation of Mn^{III} and subsequent hydrolysis of the Mn^{IV} species formed.

The extensive chemistry of manganese does not permit the determination of the film composition from voltammetric data alone. Film formation is not visible to the naked

View Article Online

Published on 01 January 1983. Downloaded by Michigan State University on 22/01/2016 01:09:22.

eye, while the chemical instability of the species in the electrolyte does not permit detection by microscopic examination after open-circuiting. The presence of sulphate is not essential for formation of this inhibiting layer. A voltammogram similar to that in fig. 2 was observed for the oxidation of Mn^{II} in 6 mol dm^{-3} $HClO_4$ in the absence of sulphate. Also current inhibition is not avoided by working in 7.5 mol dm^{-3} H_2SO_4, although this has been a commonly used medium for the Mn^{III}/Mn^{III} system.[2, 24, 31, 32]

Because of film formation the potential region available for determination of the kinetic parameters (α_a, k_s) of the anodic charge-transfer process is very limited. Application of the anodic version of eqn (1) is not feasible. Kinetic data have been obtained from Allen–Hickling[48] plots [eqn (6)] of the current–potential data of the combined oxidation–reduction voltammograms recorded during the reaction-order studies ($[Mn^{II}] = 1.4$-198.4 mmol dm^{-3}, $[Mn^{III}] = 2.0$ mmol dm^{-3}, $w = 314$ radian s^{-1}). The $[Mn^{II}]$ range was spanned in nine steps. The original voltammograms are not shown, and two typical Allen–Hickling plots derived from the data using eqn (6) are shown in fig. 7:

$$\ln\{I/[(1-I/I_{L,\,Mn^{II}})-(1+I/I_{L,\,Mn^{III}})\exp-F\eta/RT]\} = \ln i_0+\alpha_a F\eta/RT. \qquad (6)$$

Eqn (6) holds for all values of overpotential but does assume that $\alpha_a+\alpha_c = 1$. This assumption is certainly valid for the Mn^{III}/Mn^{II} system in 6.15 mol dm^{-3} H_2SO_4 at the oxide-covered platinum surface at small η, since the system was observed to give a good Nernstian response. Within the concentration range over which rest potentials were recorded ($[Mn^{III}]/[Mn^{II}] = 0.005$-$1.43$, 16 steps) the Nernstian slope (RT/F) was 0.0247 ± 0.0005 with $E_f^{\ominus} = 0.904\pm0.002$ V (from a least-squares plot).

In fig. 7, on the anodic branch, linear plots of uniform gradient are observed for $\eta < 0.2$ V, from which, for the 9 solutions investigated, α_a and k_s were determined as 0.74 ± 0.06 and $(2.1\pm0.3)\times10^{-6}$ cm s^{-1}. The true electrode area was again 0.301 cm^2. The α_a value is of the magnitude expected from the previous α_c values, but is considerably higher than that reported by Bishop and Cofré for Mn^{II} oxidation in 7.5 mol dm^{-3} H_2SO_4. However, as demonstrated in fig. 7 there is a marked change in slope (decrease in α_a) of the linear plot at overpotentials corresponding to the onset of film formation. This change is apparent even for the more dilute Mn^{II} solutions, where film formation is not directly observable (no region II) on the oxidation voltammograms, and can result in erroneous determination of α_a and k_s (i_0).

In the immediate context of the electrolytic generation of Mn^{III}, the important significance of the current-inhibiting film is that it greatly increases the overpotential required to achieve the maximum rate of Mn^{III} formation. This effect becomes more severe with increasing $[Mn^{II}]$, *e.g.* for a solution 0.2 mol dm^{-3} in Mn^{II} and 2 mmol dm^{-3} in Mn^{III} the extra overpotential is *ca.* 0.45 V.

[1] H. Diebler and N. Sutin, *J. Phys. Chem.*, 1964, **68**, 174.
[2] K. J. Vetter and G. Manecke, *Z. Phys. Chem.*, 1950, **195**, 270.
[3] J. I. Watters and I. M. Kolthoff, *J. Am. Chem. Soc.*, 1948, **70**, 2455.
[4] R. Belcher and T. S. West, *Anal. Chem. Acta*, 1952, **6**, 322.
[5] W. C. Purdy and D. N. Hume, *Anal. Chem.*, 1955, **27**, 257.
[6] H. V. K. Udupa, *Trans. Soc. Adv. Electrochem. Sci. Technol.*, 1976, **11**, 143.
[7] G. A. Kokarev, M. Ya. Fioschin, E. V. Gromova and A. T. Sorokovykh, *Elektrokhimiya*, 1981, **17**, 1380.
[8] W. A. Waters, *Quart. Rev. Chem. Soc.*, 1958, **12**, 296.
[9] C. C. Liang, in *Encyclopedia of Electrochemistry of the Elements*, ed. A. J. Bard (Marcel Dekker, New York, 1973), chap. 1-6, p. 349.
[10] A. Moussard, J. Brent, F. Jolas, M. Pourbaix and J. Von Muylder, in *Atlas of Electrochemical Equilibria in Aqueous Solution*, ed. M. Pourbaix (Pergamon Press, London, 1966), p. 286.

View Article Online

[11] F. A. Cotton and G. Wilkinson, *Advanced Inorganic Chemistry* (Interscience, New York, 2nd edn, 1966), p. 837.
[12] C. F. Wells, *Nature* (*London*), 1965, **205**, 693.
[13] R. G. Selim and J. J. Lingane, *Anal. Chim. Acta*, 1959, **21**, 539.
[14] G. Davies, *Coord. Chem. Rev.*, 1960, **1**, 199.
[15] J. E. Harrar and L. P. Rigdon, *Anal. Chem.*, 1969, **41**, 758.
[16] A. N. Campbell, *Trans. Faraday Soc.*, 1926, **22**, 46.
[17] A. R. J. P. Ubbelohde, *J. Chem. Soc.*, 1935, 1605.
[18] P. Tutundžic and S. Mladenović, *Anal. Chim. Acta*, 1955, **12**, 382, 390.
[19] D. Narasingasa Solanki and M. Prabhanjanmurty, *J. Indian Chem. Soc.*, 1942, **19**, 473.
[20] A. J. Fenton and N. H. Furman, *Anal. Chem.*, 1960, **32**, 748.
[21] R. I. Agladze and N. I. Kharabadze, *Tr. Gruz. Politekh. Inst.*, 1968, **5**, 22 (*Chem. Abstr.*, **71**, 26939).
[22] R. P. Buck, *Anal. Chem.*, 1963, **35**, 692.
[23] R. P. Buck, *Anal. Chim. Acta*, 1963, **35**, 592.
[24] E. Bishop and P. Cofré, *Analyst* (*London*), 1981, **106**, 429.
[25] J. Barek, A. Berka and K. Jakubec, *Michrochem. J.*, 1979, **24**, 454.
[26] G. A. Brydon and G. F. Atkinson, *Anal. Chim. Acta*, 1970, **51**, 539.
[27] I. M. Kolthoff and E. Jacobsen, *Microchem, J.*, 1957, **1**, 3.
[28] I. M. Kolthoff and J. I. Watters, *Ind. Eng. Chem.*, (*Anal.*), 1943, **15**, 8.
[29] D. R. Rosseinsky and R. J. Hill, *J. Chem. Soc., Dalton Trans.*, 1972, 715.
[30] J. Y. Welsh, *Electrochem. Technol.*, 1967, **5**, 504.
[31] J. A. Lee, W. C. Maskell and F. L. Tye, *J. Electroanal. Chem. Interfacial Electrochem.*, 1980, **110**, 145.
[32] R. Guidelli and G. Piccardi, *Electrochim. Acta*, 1968, **13**, 99.
[33] D. R. Rosseinsky and R. J. Hill, *Trans. Faraday Soc.*, 1974, **70**, 1140.
[34] A. C. Makrides, *J. Electrochem. Soc.*, 1966, **113**, 1158.
[35] W. Schmickler, *J. Electroanal. Chem. Interfacial Electrochem.*, 1977, **82**, 65.
[36] A. I. Vogel, *Quantitative Inorganic Analysis* (Longmans Green, London, 3rd edn, 1961), p. 327.
[37] L. Ciavatta and M. Grimaldi, *J. Inorg. Nuclear, Chem.*, 1969, **31**, 3071.
[38] S. Shibata, *Electrochim. Acta*, 1977, **22**, 175.
[39] J. W. Schultze and K. J. Vetter, *Electrochim. Acta*, 1973, **18**, 889.
[40] S. Gilman, in *Electroanalytical Chem.*, ed. A. J. Bard (Marcel Dekker, New York, 1967), vol. 2, p. 111.
[41] K. J. Vetter and J. W. Schultze, *Ber. Bunsenges. Phys. Chem.*, 1973, **77**, 945.
[42] A. Damjanovic and A. T. Ward, in *Electrochemistry The Past Thirty and the Next Thirty Years*, ed. H. Bloom and F. Gutman (Plenum Press, New York, 1977), p. 89.
[43] D. Gilroy, *J. Electroanal. Chem. Interfacial Electrochem.*, 1977, **83**, 329.
[44] T. Biegler, D. A. J. Rand and R. Woods, *J. Electroanal. Chem. Interfacial Electrochem.*, 1971, **29**, 269.
[45] T. Biegler, *J. Electrochem. Soc.*, 1969, **116**, 1131.
[46] V. S. K. Nair and G. H. Nancollas, *J. Chem. Soc.*, 1959, 3934.
[47] C. J. Hallada and G. Atkinson, *J. Am. Chem. Soc.*, 1961, **83**, 3759.
[48] P. L. Allen and A. Hickling, *Trans. Faraday Soc.*, 1957, **53**, 1626.

(PAPER 2/669)

Published on 01 January 1983. Downloaded by Michigan State University on 22/01/2016 01:09:22.